

# THE DØ EXPERIMENT AT THE FERMILAB TEVATRON COLLIDER <sup>1</sup>

GREGORY R. SNOW  
*University of Michigan*  
*Ann Arbor, Michigan 48109, USA*

for the DØ Collaboration

## ABSTRACT

The DØ Experiment is a new, large multipurpose experiment at the Tevatron Proton-Antiproton Collider at the Fermi National Accelerator Laboratory. The DØ detector is described. From the analysis of data taken during August–October, 1992, a selection of preliminary physics results will be given on inclusive jet production, direct photon production, and the production and decay properties of the  $W$  and  $Z$  bosons. The search for the top quark in the dilepton and lepton + jets channels is also discussed.

## 1. The DØ Detector

The DØ Experiment is a collaboration of 36 universities and laboratories from 7 countries. The primary goal of the DØ Experiment[1, 2] is the precision study of high mass, large transverse momentum phenomena with particular emphasis on measurements of leptons (electrons and muons), photons, jets (clusters of produced particles), and missing transverse momentum indicative of penetrating particles (such as neutrinos). To accomplish this goal, the detector design stresses uniform, hermetic, fine-grained calorimetry, large solid angle coverage and excellent muon detection. The Detector is shown in Fig. 1. It includes three major components: the outer Muon System, the inner Central Tracking System, and the liquid argon Calorimeter System.

### 1.1. Muon System

The Muon System[3] consists of five iron toroids, 1.1–1.5 meters thick, and three layers of proportional drift tube (PDT) chambers. The central toroid surrounds the calorimeter and covers angles down to 45°. The end toroids and the small angle muon system cover the forward region down to 5°. Thus there is full muon coverage for  $|\eta| \leq 3.2$ . The momentum of a muon is determined by using the PDT chambers to measure the deflection of the muon trajectory in the 1.9 T steel toroids. The momentum resolution, typically 20%, is dominated by multiple scattering for momenta  $< 80$  GeV/ $c$ . The combined calorimeter plus toroid thickness varies from 14  $\lambda$  in the central region to 19  $\lambda$  in the end regions. This thickness reduces backgrounds from hadronic punchthroughs to a negligible level[4].

### 1.2. Central Tracking System

The Central Tracking System[5], shown in Fig. 2, consists of four main com-

---

<sup>1</sup>Presented at the VII International Symposium on Very High Energy Cosmic Ray Interactions, June 22–27, 1992, Ann Arbor, Michigan.

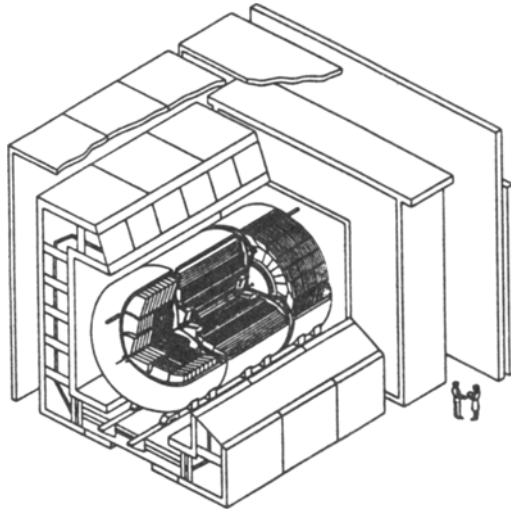


Figure 1: The DØ Detector

ponents: Vertex Chamber, Transition Radiation Detector, Central Drift Chamber and two sets of Forward Drift Chambers.

The Vertex Chamber[6] has three cylindrical layers of jet-type cells, and every cell in a layer has eight sense wires. It provides precision charged particle tracking with good azimuthal spatial resolution ( $60 \mu\text{m}$ ) and good two-track resolution ( $0.6 \text{ mm}$ ). Charge division is used to measure the axial coordinate with a resolution of about  $1 \text{ cm}$ . The chamber is also used to find secondary vertices, and reject photon conversions which can give a fake electron signal.

The Transition Radiation Detector[7] provides additional rejection of pions in the identification of central electrons. It has three cylindrical layers, each layer consisting of a set of polypropylene foils at the inner radius, and a radial drift X-ray detector at the outer radius. A pion rejection factor of 50 was achieved in a test beam for an electron efficiency of 90%.

The Central Drift Chamber[8] has four cylindrical layers of jet-type cells, and every cell in a layer has seven sense wires. Its azimuthal spatial resolution is  $150 \mu\text{m}$ . The axial position of tracks is measured with delay lines, with a resolution of  $4 \text{ mm}$ . Measurements of  $dE/dx$  are used to help identify conversions.

The Forward Drift Chambers[9] cover angles down to  $5^\circ$ , and include two types of units. The  $\Phi$  units have radial sense wires, with 16 measurements along each track. The  $\Theta$  units have sense wires oriented transversely to the beam, with 8 measurements along each track in each of the two units. The spatial resolution

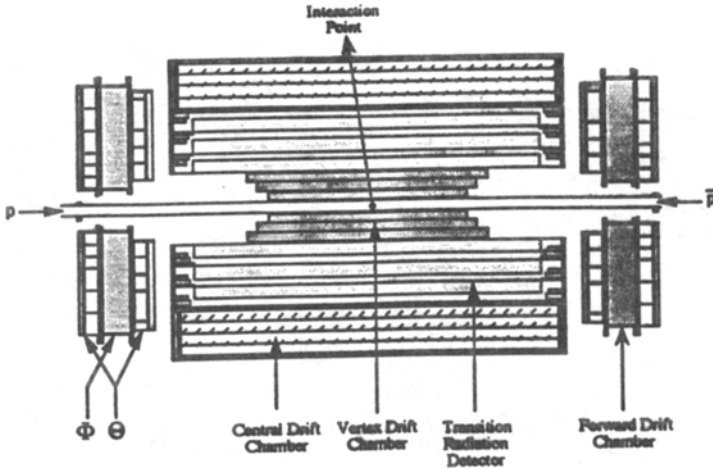


Figure 2: The DØ Central Tracking System.

in each unit is  $200 \mu\text{m}$ .

### 1.3. Calorimeter System

The DØ calorimeters are sampling calorimeters using uranium as the absorbing material and liquid argon as the sampling medium. The use of uranium not only leads to a compact calorimeter design, but it helps in equalizing the calorimeter response to electrons and hadrons. This is important for minimizing the fluctuations in the observed energies of jets, whose particle content may vary. Liquid argon is used as the active ionization medium because of its ease of calibration, its stability and uniformity of response, and its radiation hardness.

The DØ Calorimeter System [10, 11] shown in Fig. 3, consists of a cylindrical Central Calorimeter and two End Calorimeters covering angles down to within  $1^\circ$  of the beamline. Each of the three calorimeters contains an electromagnetic (e.m.) section with thin uranium plates, a fine hadronic section with thick uranium plates, and a coarse hadronic section with very thick copper or steel plates. Printed circuit boards with segmented detection pads are interleaved between the absorber plates to detect the ionization in the liquid argon. All of the DØ calorimeter modules use a uniform technology to facilitate the relative calibration between modules. The calorimeters are designed with minimal cracks and other uninstrumented regions in order to provide essentially hermetic coverage.

The calorimeters are finely segmented both longitudinally and transversely. Longitudinally, each e.m. section is divided into 4 readout depths (for a total of  $21 X_0$ ), and the hadronic sections are divided into 4-5 depths (for a total of

## DØ LIQUID ARGON CALORIMETER

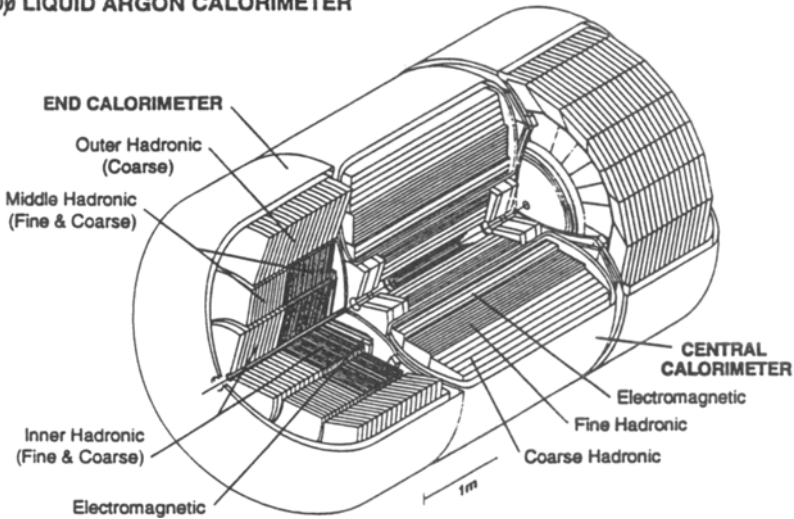


Figure 3: The DØ Calorimeter System.

7–9  $\lambda$ ). The transverse segmentation is  $0.1 \times 0.1$  for  $\Delta\eta \times \Delta\phi$ , except in the third e.m. longitudinal section (where shower max occurs), where the segmentation is increased to  $0.05 \times 0.05$  for better shower position resolution. The readout cells are arranged in semi-projective towers.

Typical e.m. and hadronic calorimeter modules have been extensively tested with electrons and pions from 2 to 150 GeV in a test beam at FNAL[10, 12, 13]. The fractional energy resolution of electrons in the calorimeters is  $15\%/\sqrt{E}$ , and of pions is  $50\%/\sqrt{E}$ . The spatial position resolution for electrons is 1–2 mm, for energies above 50 GeV. Using the transverse and longitudinal shower shape information from the e.m. and hadronic modules, a pion rejection factor of greater than 1000 has been measured for a 95% electron efficiency. The  $e/\pi$  response of the calorimeter system is energy dependent but varies within the range 1.02–1.05.

The missing transverse energy,  $\cancel{E}_T$ , resolution of the DØ Calorimeter System, important for new particle searches and the precision measurement of the mass of the  $W$  boson, is excellent because of the calorimeter's hermeticity and uniformity. Using minimum bias collider data, the  $\cancel{E}_T$  resolution has been shown to be 2–4 GeV for scalar  $E_T$  in the range 50–150 GeV.

#### 1.4. Trigger

The DØ uses a Trigger System[14] based on 3 successive decisions. The initial (Level 0) trigger uses scintillation counters on both sides of the interaction point to determine if a beam-beam interaction occurred during a particular beam crossing. This rate depends on the luminosity, but is typically 100 kHz. The next

(Level 1) trigger[15] is a hardware trigger using information from the Muon System and Calorimeter. Part of the calorimeter signal is split off, and e.m. and hadronic energy is summed separately for  $\Delta\eta \times \Delta\phi = 0.2 \times 0.2$  trigger towers. The Level 1 trigger can then make cuts on various combinations of counts of EM and jet towers above  $E_T$  thresholds, missing and total scalar  $E_T$  above thresholds, and the number of muons. The Level 1.5 trigger uses more detailed information from the muon chambers to make a  $P_T$  cut for muon triggers. The Level 1/1.5 rate at the present time is 70 Hz, which will be increased to 200 Hz in the near future.

The Level 2 trigger[16] is a software filter running on a farm of VAX 4000/60 microprocessors. There the full event readout is used, and algorithms identify and measure electrons, photons, jets and muons, and calculate more accurately the event missing  $E_T$  and total scalar  $E_T$ . The filter then makes cuts on various combinations of these objects, with various thresholds. The events passing Level 2 are written to tape. The Level 2 event rate is currently 2 Hz, which will be increased to 4 Hz in the near future.

### 1.5 Operation at the Tevatron Collider

The DØ Detector saw its first  $p\bar{p}$  collisions at the Fermilab Collider in May, 1992, when commissioning of the detector began with detailed studies of the trigger, backgrounds, and various detector elements. In August, 1992, we started our first physics data taking run with this detector. By the end of October, 1992, we had accumulated data on tape representing an integrated luminosity of  $1.1 \text{ pb}^{-1}$ . All of the results presented in the next section are based on data from that sample, and are preliminary.

## 2. Physics Analysis Highlights

### 2.1 Electroweak

Both  $W \rightarrow \mu\nu$  and  $W \rightarrow e\nu$  have been detected in DØ. The search in the  $\mu$  channel[17] was performed for a luminosity of  $410 \text{ nb}^{-1}$ . The muons in this sample have  $|\eta| < 1.0$ , have a match to a central detector track, and have  $P_T > 20 \text{ GeV}/c$ . QCD background has been eliminated by requiring that the muon track be isolated in the calorimeter, and cosmic ray background has been reduced using drift timing from the muon chambers. The search in the e channel[18] was performed for a luminosity of  $1.1 \text{ pb}^{-1}$ . The electrons were identified as e.m. clusters having  $< 10\%$  of their energy in the hadronic calorimeter sections, having a transverse and longitudinal cluster shape  $\chi^2$  which agrees with test beam expectations[19], and being isolated from the rest of the event. In addition, a track was required to be found in the tracking chambers pointing to the calorimeter cluster. The missing  $P_T$  is  $> 20 \text{ GeV}/c$  for both  $\mu$  and e samples. Figs. 4a and 4b show the  $W$  transverse mass for the  $\mu$  and e samples, respectively. Monte carlo predictions and fits, shown by solid curves in each figure, are used to determine the  $W$  mass and width.

In the  $\mu$  sample, the observed number of events is 25, including 6 background events, for a total of 19  $W$  events, in good agreement with the expected number

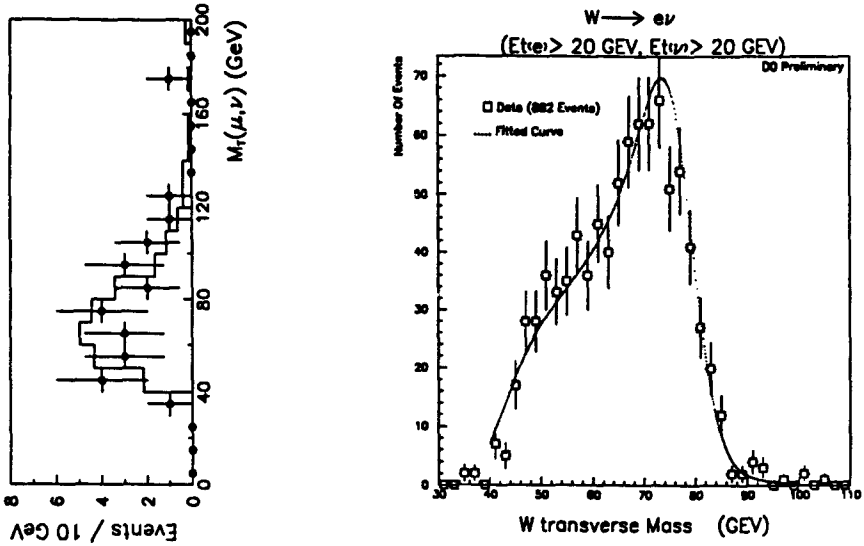


Figure 4: a)  $W$  transverse mass for  $W \rightarrow \mu\nu$  events. b)  $W$  transverse mass for  $W \rightarrow e\nu$  events. In both figures the points are data and the solid curve is Monte Carlo.

of  $22 \pm 5$  events. The cross section for  $W$  production times the branching ratio for  $W \rightarrow e\nu$  is calculated for the  $e$  sample (882 events) to be  $2.3 \pm 0.5$  nb, in good agreement with published values.

A clean  $Z \rightarrow ee$  peak is seen in the data[18]. Fig. 5 shows the invariant mass distribution for di-electrons, in the  $1.1 \text{ pb}^{-1}$  data sample, with both electrons having  $E_T > 20$  GeV. For this distribution, only one of the electrons was required to have a matching track. A Breit-Wigner fit to the 72 events, shown in Fig. 5, gives a peak of about 86 GeV. This is using the energy scale calibration directly from the test beam, without any corrections for the collider data, and is currently estimated to be correct to about 5%. Studies are underway to obtain a more precise energy scale. This must be done before a value for the  $W$  mass will be quoted.

### 2.2 Top

The top quark has been shown to have a mass greater than  $89 \text{ GeV}/c^2$  by the CDF collaboration. Hence, for present searches at the Tevatron Collider, top quark production and decay are expected to proceed via:

$$p\bar{p} \rightarrow t\bar{t} \rightarrow W^+W^-b\bar{b}$$

with the  $W$  bosons decaying into either lepton + neutrino, or jets. Thus in the final

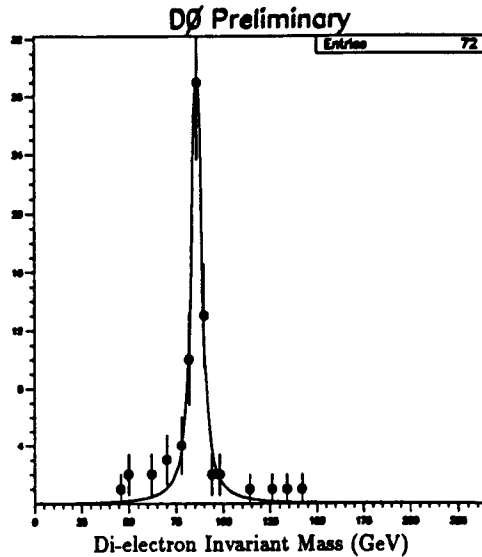


Figure 5: Di-electron invariant mass distribution, with a Breit-Wigner fit.

state one expects:

dileptons + jets +  $\cancel{E}_T$ , or  
 lepton + jets +  $\cancel{E}_T$ , or  
 all jets.

The search for top exploits the DØ detector's large angular acceptance for electrons, jets and muons, and its excellent missing  $E_T$  resolution.

Searches for the top quark were performed in the di-electron channel[20], the electron+muon channel[20], and the electron+jets channel[21] using the  $1.1 \text{ pb}^{-1}$  data sample. No events were detected which satisfied the relevant kinematic cuts for each channel, which, given the luminosity in the sample, was consistent with expectations for a top quark mass heavier than  $80 \text{ GeV}/c$ . The  $e+\mu$  channel is regarded as the "discovery" channel, due to low backgrounds from other sources. The Tevatron Collider runs which are scheduled into 1994 are expected to provide  $100 \text{ pb}^{-1}$  of integrated luminosity, and the top quark searches with this data sample should be sensitive to a mass extending to about  $150 \text{ GeV}/c^2$ .

### 2.3 QCD

DØ, with its hermetic and finely segmented calorimeters, is ideal for a study of jet distributions. A particularly advantageous feature of DØ is its ability to trigger on jets all the way down to  $\eta = 3.2$ . The preliminary inclusive jet cross section[22] is shown in Fig. 6 for a data sample corresponding to  $130 \text{ nb}^{-1}$  of luminosity. The jets were reconstructed using a cone algorithm, with the cone radius = 0.7 (in  $\eta-\phi$  space). The band in Fig. 6 is the upper and lower limit for the cross section includ-

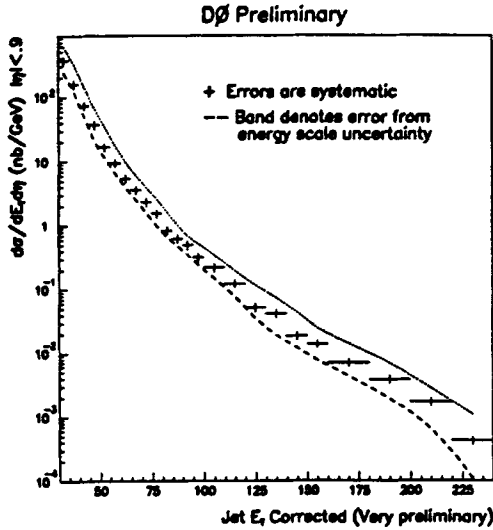


Figure 6: Inclusive jet cross section vs. jet  $E_T$ .

ing the current energy scale uncertainty. We have also measured the 2-jet double differential cross-sections[23] out to rapidities of 3.2 where the structure functions have considerable impact upon the results.

The full coverage of the DØ calorimeters to  $|\eta| = 4.0$  and their fine segmentation and good energy resolution allow us to make a good measurement of direct photon production. Direct photons in the central region ( $|\eta| < 0.9$ ) and in the  $P_T$  range of 14–90 GeV/c were searched for in the same  $130 \text{ nb}^{-1}$  sample of data used for the jet studies. The photons were required to have a transverse and longitudinal shape  $\chi^2$  which agrees with test beam expectations[19], to be isolated in a cone of  $R = 0.4$  from the rest of the event, and to not have a track nearby. Backgrounds due to  $\pi^0$  decays which pass the cuts were estimated through study of the ratio of 1-photon and 2-photon conversions in the tracking material, and by Monte Carlo simulations. Both methods are in agreement, finding that the fraction of photons in the candidate sample is  $0.42 \pm 0.14$ . The resulting direct photon cross section[24] is shown in Fig. 7. The error bars include an estimate of the systematic errors. It is seen that the data agree well with a next-to-leading-order (NLO) calculation[25].

DØ has also detected many events in which  $W$ 's are produced in association with jets[26]. This process provides a good test of NLO QCD calculations and a measurement of the strong coupling constant  $\alpha_s$ .

#### 2.4 Other Physics Analyses

The excellent muon coverage of the DØ detector for the full solid angle ( $|\eta| < 3.2$ ) and the ability to identify muons within jets lend themselves to the study



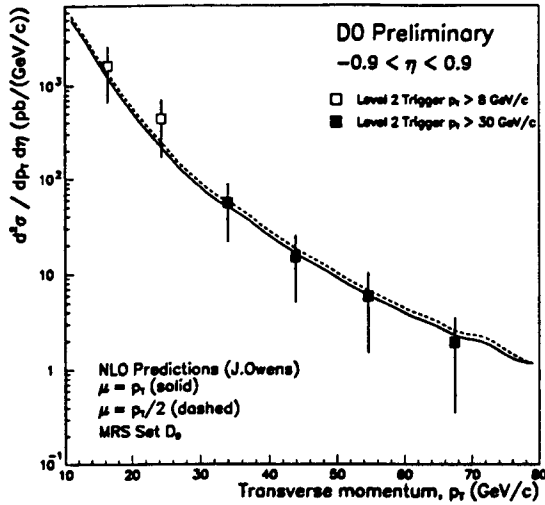


Figure 7: Direct photon cross section vs. photon  $P_T$ .

of  $b$  quark decays. The  $P_T$  spectrum for inclusive single muon production[27] is shown in Fig. 8. At least one jet was required to be near the muon track for events in this distribution. Also shown in Fig. 8 is the Monte Carlo expectation from  $b$  and  $c$  quarks, normalized to the total number of events. It is seen that the shapes agree well.

Because of the  $D\bar{D}$  detector's excellent  $\cancel{E}_T$  resolution and acceptance for multijets and leptons, it will play an important roll in the search for particles which exist in the minimal supersymmetric extension of the Standard Model. For example, gluinos and squarks are produced either via "direct decay" into the lightest neutralino (with large  $\cancel{E}_T$  and high  $E_T$  jets) or via the "cascade decay" through several supersymmetric particles and finally into the lightest neutralino (with less  $\cancel{E}_T$ , softer jets, and possible leptons). Searches for squarks and gluinos[28] are in progress.

$D\bar{D}$  has also searched for leptoquarks which carry both color quantum numbers and lepton quantum numbers, and can decay, for example, into a lepton and a quark. In composite models, leptoquarks are the natural result of different combinations of the constituents of quarks and leptons. A search was done[29] for scalar leptoquarks, looking for events with 2 electrons and 2 jets, with a data sample corresponding to  $0.8 \text{ pb}^{-1}$ . Assuming a 100% branching ratio into the electron + quark decay mode, we have set a lower limit on a leptoquark mass of  $74 \text{ GeV}/c^2$ , at

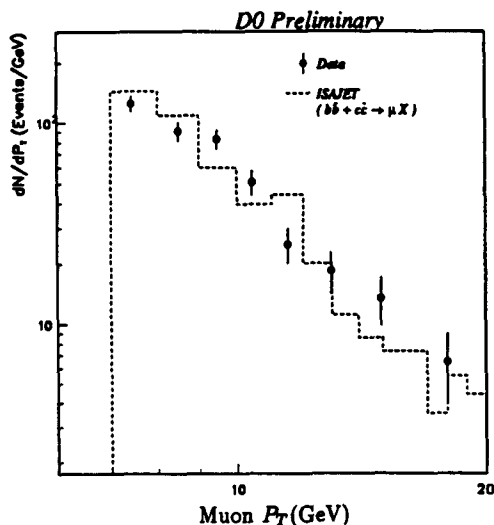


Figure 8: Inclusive muon  $P_T$  spectrum.

95% CL.

### 3. Conclusion

The DØ Detector has been installed at the Fermilab Tevatron Collider and is currently taking physics data. Preliminary physics results, based on the first three months of data taking after commissioning, have emerged in the areas of electroweak, QCD,  $B$  physics, top and new particle searches. We look forward to accumulating further luminosity for our precision studies and searches for rare processes.

### 4. Acknowledgements

I am indebted to the DØ physics analysis groups and the many physicists who prepared preliminary results for the November, 1992, DPF meeting at Fermilab. I especially thank Dr. Ron Madaras for letting me draw on his excellent summary of results for this write-up. This work was supported by the U.S. Department of Energy and the National Science Foundation.

### 5. References

1. Design report for the DØ Experiment at the Fermilab Antiproton-Proton Collider, Fermilab, November 1984 (unpublished).

2. P.D. Grannis, in the *Proceedings of Les Rencontres de Physique de la Vallée d'Aoste on Results and Perspectives in Particle Physics*, La Thuile, March 1987, edited by M. Greco (Editions Frontieres, 1987) p. 253.
3. C. Brown, *et al.*, *Nucl. Instr. and Meth.* **A279** (1989) 331; J.M. Butler, *et al.*, *Nucl. Instr. and Meth.* **A290** (1990) 122.
4. D. Green, *et al.*, *Nucl. Instr. and Meth.* **A244** (1985) 356.
5. A.R. Clark *et al.*, *Nucl. Instr. and Meth.* **A279** (1989) 243.
6. A.R. Clark *et al.*, *Nucl. Instr. and Meth.* **A315** (1992) 193.
7. J.F. Detoeuf *et al.*, *Nucl. Instr. and Meth.* **A265** (1988) 157.
8. T. Behnke, Ph.D. Thesis, SUNY, Stony Brook (1989); D. Pizzuto, Ph.D. Thesis, SUNY, Stony Brook (1991).
9. R.E. Avery *et al.*, DØ Note 1567 to be published in the *IEEE Trans. in Nuc. Sci.*
10. H. Aihara *et al.*, LBL-31378 (July 1992), to be published in *Nucl. Instr. and Meth.*
11. J. Christenson, to be published in the *Proceedings of the Third International Conference on Calorimetry in High Energy Physics*, Corpus Christi, Texas, September, 1992.
12. S. Abachi *et al.*, FNAL-PUB-92/162, to be published in *Nucl. Instr. and Meth.*
13. P. Bhat, "Low Energy Response of the DØ Calorimeter and Jet Energy Measurement", to be published in the *Proceedings of the 1992 Annual Meeting of the American Physical Society Division of Particles and Fields*, Fermilab, November, 1992 (*DPF-92*)
14. Jan Guida, DØ Note 1510, to be published in the *Proceedings of the Third International Conference on Calorimetry in High Energy Physics*, Corpus Christi, Texas, September, 1992.
15. M. Abolins *et al.*, *Nucl. Instr. and Meth.* **A289** (1990) 543.
16. J. Linnemann, DØ Note 1519, to be published in the *Proceedings of the Conference on Computing in High Energy Physics*, Annecy, France, September, 1992, and also *DPF-92*.
17. D. Wood, "*W* and *Z* Decays to Muons at DØ", to be published in *DPF-92*.
18. N. Graf, "*W* and *Z* Decays to Electrons at DØ", to be published in *DPF-92*.
19. M. Narain, "Electron Identification in the DØ Detector", to be published in *DPF-92*.
20. R. Partridge, "Search for the Top Quark in Dilepton Events with DØ", to be published in *DPF-92*.
21. B. Klima, "Search for the Top Quark in Electron+Jets Events in DØ", to be published in *DPF-92*.

22. R. Astur, "Inclusive Jet Distributions at  $D\bar{D}$ ", to be published in *DPF-92*.
23. G. Blazey, "Dijet Differential Distributions", to be published in *DPF-92*.
24. G.R. Snow, "Direct Photon Production at  $D\bar{D}$ ", to be published in *DPF-92*.
25. H. Baer, J. Ohnemus, J.F. Owens, *Phys. Lett.* **B234** (1990) 127, and private communication.
26. J. Yu, "W+Jet Production with  $D\bar{D}$ ", to be published in *DPF-92*.
27. K. Bazizi, "Inclusive Single Muon Production with  $D\bar{D}$ ", to be published in *DPF-92*.
28. M. Paterno, "A Search for Squarks and Gluinos with  $D\bar{D}$ ", to be published in *DPF-92*.
29. W. Merritt, "Search for Scalar Leptoquarks in  $D\bar{D}$ ", to be published in *DPF-92*.